Acta Crystallographica Section D
Biological Crystallography
ISSN 0907-4449

Structure of native laccase from *Trametes hirsuta* at 1.8 Å resolution

Konstantin M. Polyakov,[a,b]* Tatyana V. Fedorova,[b] Elena V. Stepanova,[b] Evgeny A. Cherkashin,[b] Sergei A. Kurzeev,[b] Boris V. Strokopytov,[a] Victor S. Lamzin[c] and Olga V. Koroleva[b]

[a]V. A. Engelhardt Institute of Molecular Biology, Russian Academy of Sciences, Vavilova Street 32, 119991 Moscow, Russia, [b]A. N. Bach Institute of Biochemistry, Russian Academy of Sciences, Leninsky Prospect 33, 119071 Moscow, Russia, and [c]European Molecular Biology Laboratory (EMBL), c/o DESY, Notkestrasse 85, 22603 Hamburg, Germany

Correspondence e-mail: kostya@eimb.ru

Received 29 January 2009
Accepted 31 March 2009

PDB Reference: laccase, 3fpx, r3fpxsf.

This paper describes the structural analysis of the native form of laccase from *Trametes hirsuta* at 1.8 Å resolution. This structure provides a basis for the elucidation of the mechanism of catalytic action of these ubiquitous proteins. The 1.8 Å resolution native structure provided a good level of structural detail compared with many previously reported laccase structures. A brief comparison with the active sites of other laccases is given.

1. Introduction

Laccase (EC 1.10.3.2; *n*-diphenol:oxygen oxidoreductase) belongs to a class of copper-containing proteins and catalyzes the four-electron reduction of molecular oxygen by various organic and inorganic compounds, skipping the stage of hydrogen peroxide formation (the second substrate, oxygen, is endogenous). Laccases have broad substrate specificity which can be further increased by using redox mediators and enhancers, although in this case the reaction takes place through the formation of free radicals. Laccases can oxidize various nonphenolic compounds, also in the presence of redox mediators and enhancers. In addition, they can perform direct electron exchange between an electrode and the enzyme active site (Shleev, Jarosz-Wilkolazka *et al.*, 2005; Shleev, Tkac *et al.*, 2005).

The properties of laccases mentioned above give rise to numerous applications in various branches of biotechnology, *e.g.* biodegradation and detoxification (Gianfreda *et al.*, 1999; Gianfreda & Rao, 2004; Amitai *et al.*, 1998; Torres *et al.*, 2003), organic synthesis, the preparation of new pharmaceutical drugs, energy conversion (Barton *et al.*, 2002; Marzorati *et al.*, 2005; Baratto *et al.*, 2006; Riva, 2006), the textile industry, drink preservation and stabilization, and many others (Couto & Toca-Herrera, 2006*a*,*b*; Riva, 2006).

Laccases contain four coppers assembled in their active sites. Other copper-containing enzymes, *e.g.* ascorbate oxidase and ceruloplasmin, have a similar organization of active sites and properties, but only laccases can participate in direct bioelectrocatalysis. They contain at least one type (T1) of copper bound as a mononuclear centre, which shows a characteristic intense absorption band at 600 nm. The type 2 (T2) site behaves as a mononuclear site with normal spectral features and is EPR active. Unlike type 1 copper and type 2 copper, type 3 copper is not detected in the EPR spectrum because of a strong antiferromagnetic interaction. One T2 and two type 3 (T3α and T3β) sites form a trinuclear site which is responsible for the reduction of dioxygen (Solomon *et al.*, 1996; Messerschmidt *et al.*, 1992; Bento *et al.*, 2005).

To date, several schemes for the catalytic events in the active site of laccases have been proposed. Unfortunately, there is still no rigorous proof of the formation of some of the intermediates suggested by various authors (Solomon *et al.*, 1992, 1996; Yoon *et al.*, 2007). The function of the T2/T3 copper centre remains unclear. This suggests that further crystallographic research is necessary in order to clarify the catalytic mechanism.

This paper describes the structure and crystallographic refinement of the highly redox-capable laccase from *Trametes hirsuta* at 1.8 Å resolution. A brief comparison with related laccase structures from the Protein Data Bank (Piontek *et al.*, 2002; Bertrand *et al.*, 2002; Lyashenko, Bento *et al.*, 2006) is made.

2. Methods

2.1. Enzyme production and purification

A strain producing extracellular laccase, *T. hirsuta* 072, was obtained from the Komarov Botanical Institute of the Russian Academy of Sciences (St Petersburg). The laccase was isolated from the culture liquid after submerged cultivation of *T. hirsuta* 072 and purified as described by Koroljova *et al.* (1998). The homogeneity of the enzyme was confirmed by SDS–PAGE (12.6% acrylamide in 0.2 *M* Tris–glycine buffer pH 8.3) under denaturing conditions. The amino-acid sequence was obtained from the cDNA using the polymerase chain reaction (PCR) technique (GenBank accession code gi:46578390).

The syringaldazine oxidase activity of the laccase was determined as previously reported by Leonowicz & Grzywnowicz (1981). The enzyme activity is expressed as international units (U), where 1 U corresponds to the formation of 1 µmol of product per minute at 298 K.

2.2. Primary sequence determination

PCR was carried out using Tertsik-2 equipment from DNA Technologies, Russia. The total mixture volume was 25 µl (placed in 0.5 ml microtest tubes) containing 60 m*M* Tris–HCl pH 8.5 at 298 K, 1.5 m*M* $MgCl_2$, 25 m*M* KCl, 10 m*M* $(NH_4)_2SO_4$, 10 m*M*-mercaptoethanol, 0.2% Triton X-100, 100 µl of each dNTP and 1 µl of each primer. The reaction was performed using the following protocol: initial denaturation at 368 K for 2 min followed by 30 cycles consisting of denaturation at 368 K for 1 min, annealing at 329–361 K for 1 min and elongation at 345 K for 2 min; final elongation was performed for 10 min at 345 K.

Electrophoresis of PCR products was performed in TAE buffer using 1% agarose gel at an electric field voltage of 2–3 V cm^{-1}. The DNA sample was mixed with 10× buffer for drawing (0.1% Bromophenol Blue, 50% glycerol, 0.1 *M* EDTA pH 8.0) in a 9:1 ratio. Visualization of the obtained fragments was carried out using ethidium bromide (EtBr) at 260 nm wavelength.

DNA sequencing was performed at the Inter-Institute GENOM Centre in the Institute of Molecular Biology using ABI PRISM BigDye Terminator v.3.1, with subsequent analysis of the reaction products on an ABI PRISM 3100-Avant automatic DNA sequencer. The amino-acid sequence was obtained from chromosome cloning (GenBank accession code gi:183178982).

Table 1
Data-collection and refinement statistics.

Values in parentheses are for the outer shell (1.86–1.84 Å).

Space group	$P2_12_12_1$
Unit-cell parameters (Å)	a = 50.65, b = 74.01, c = 124.83
Resolution (Å)	19.0–1.84
$I/\sigma(I)$	19.8 (2.7)
Completeness (%)	94.7 (81.3)
Total reflections	215595
Unique reflections	46382
R_{merge}	0.074 (0.58)
Redundancy	4.6
R (%)	18.0
R_{free} (%)	23.2
No. of atoms	4254
Protein atoms	3804
Cu ions	4
Sugars	164
Water molecules	275
Phosphate ions	5
R.m.s.d. bonds (Å)	0.021
R.m.s.d. angles (°)	1.79
Mean ADP for protein atoms (Å^2)	31.0
Mean ADP for solvent atoms (Å^2)	35.3
No. of residues in Ramachandran plot regions	
Most favoured	436
Additionally allowed	58
Generously allowed	2
Disallowed	1

2.3. Crystallization and data collection

Laccase crystals were grown by the hanging-drop vapour-diffusion method. The drop contained equal amounts of protein solution at a concentration of 30 mg ml^{-1} in 0.05 *M* potassium phosphate buffer pH 7.0 and reservoir solution containing 10% PEG 1000 and 10% PEG 8000. The dimensions of the crystals were about 0.3 × 0.5 × 1.0 mm. The crystals belonged to space group $P2_12_12_1$, with unit-cell parameters a = 50.65, b = 74.01, c = 124.83 Å. Assuming the presence of one protein molecule per asymmetric unit, the Matthews coefficient was 2.15 Å^3 Da^{-1}, suggesting that approximately 40% of the unit cell is occupied by solvent.

The data set was collected to 1.8 Å resolution on the EMBL beamline BW7A at the DESY synchrotron (Hamburg). Prior to data collection, crystals were soaked in a cryoprotectant containing reservoir solution with paraffin oil (Hampton Research, USA) for 2–10 min and flash-cooled to 100 K using an Oxford low-temperature system. The data sets were collected with a MAR CCD 165 detector at a wavelength of 1.38 Å.

The data were processed using the *HKL* suite (Otwinowski & Minor, 1997). Further scaling and reduction were performed with the *CCP*4 suite (Collaborative Computational Project, Number 4, 1994). The *TRUNCATE* program (French

& Wilson, 1978) was used to replace negative intensities with small positive values according to Bayesian statistics. The statistics of the data set are given in Table 1.

3. Results

3.1. Crystallographic refinement

MOLREP (Vagin & Teplyakov, 1997) was used to solve the structure of native laccase using the molecular-replacement method. The *T. versicolor* laccase structure (PDB code 1gyc), which had 80% identity to the target structure, was used as a starting model. Both rotation-function and translation-function searches were carried out at 4.0 Å resolution. All water molecules and sugar residues were excluded from the *T. versicolor* model structure before the molecular-replacement runs. The correct molecular-replacement solution corresponded to the highest peak both in the rotation function and translation function. The initial R value (based on calculated F_c values) was 0.350 before the start of the refinement.

Atomic positions and isotropic atomic displacement parameters (ADPs) were refined using *REFMAC* (Murshudov *et al.*, 1997). 2178 reflections (4% of the data) were used for the calculation of R_{free}. The stereochemical parameters of the model were closely monitored during crystallographic refinement.

The manual correction of problematic loop regions, bulk-solvent correction and the inclusion of additional hydrocarbon residues and water molecules using σ_A-weighted maps (Read, 1986; Murshudov *et al.*, 1997) led to R_{cryst} = 0.182 and R_{free} = 0.240 for the final laccase structure. Visual inspection of the models was carried out using the *Coot* program package (Emsley & Cowtan, 2004).

The final model contained 4254 non-H atoms with good stereochemistry. The refinement statistics are given in Table 1. A cartoon representation of the fold of the laccase molecule is shown in Fig. 1. The coordinates and structure factors for native laccase from *T. hirsuta* (PDB code 3fpx) have been deposited in the Protein Data Bank (Berman *et al.*, 2002).

3.2. Structure analysis

3.2.1. Primary sequence correction. During the crystallographic refinement, rather large discrepancies between the primary sequence and the X-ray density map were observed. The primary sequence was gradually corrected during the refinement so that several residues in the model (Gln242, Asn419, Arg423, Gly429 and Arg440) differed from the DNA-based sequence (cDNA), in which they were identified as Pro, Gly, Pro, Arg and Gln, respectively. Inconsistencies between the sequences derived from the X-ray density map and the DNA-based sequence (cDNA) have also been reported for fungal laccases (Piontek *et al.*, 2002; Ferraroni *et al.*, 2007). However, data acquisition for the full-length primary sequence allowed us to refine the primary sequence. Only one amino acid of this gene sequence, namely Pro182, does not fit to the X-ray density, which clearly indicates the presence of a valine (Val182). Since the corresponding electron densities are of high quality, a gene-sequencing error (or the expression of a natural mutant) should be assumed. Therefore, for fungal laccases with a complex intron–exon gene organization, the chromosome cloning allows the avoidance or reduction of gene-sequencing

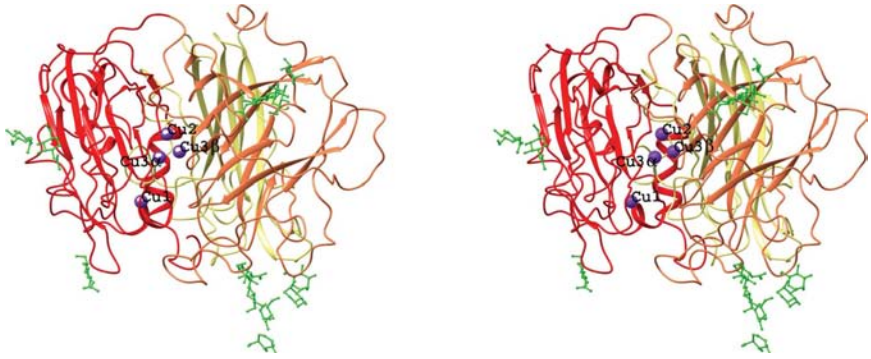

Figure 1
Stereo cartoon of the laccase three-dimensional structure. Domains 1, 2 and 3 are shown in yellow, coral and red, respectively. Cu atoms are in violet. The atoms of bound sugar residues are shown in green.

```
1234567890 1234567890 1234567890 1234567890 1234567890 1234567890
      β1                   β2          β3         β4
AVGPVADLTI TDAAVSPDGF SRQAVVVNGV TPGPLVAGNI GDRFQLNVID NLTNHTMLKS  60
   β5                                 β6         β7          α1
TSIHWHGFFQ HGTNWADGPA FINQCPISPG HSFLYDFQVP DQAGTFWYHS HLSTQYCDGL 120
   β8         α2          β9                      β10
RGPFVVYDPN DPHASRYDVD NDDTVITLAD WYHTAAKLGP RFPGGADATL INGKGRAPSD 180
      β11        β12         β13        β14        β15        β16
SVAELSVIKV TKGKRYRFRL VSLSCNPNHT FSIDGHNLTI IEVDSVNSQP LEVDSIQIFA 240
   β17           β18                    β19
AQRYSFVLDA NQAVDNYWIR ANPNFGNVGF DGGINSAILR YDGAPAVEPT TNQTTSVKPL 300
 α3                      β20  β21     β22
NEVDLHPLVS TPVPGSPSSG GVDKAINMAF NFNGSNFFIN GASFVPPTVP VLLQILSGAQ 360
          β23      β24                 β25       β26
TAQDLLPSGS VYVLPSNASI EISFPATAAA PGAPHPFHLH GHTFAVVRSA GSTVYNYDNP 420
β27 β28   α4       β29        β30      α5        β31       α6
IFRDVVSTGT PAAGDNVTIR FDTNNPGPWF LHCHIDFHLE GGFAVVMAED TPDVKAVNPV 480
      α7
PQAWSDLCPT YDALDPNDQ                                           499
```

Figure 2
Primary sequence and secondary-structure elements of *T. hirsuta* laccase.

errors. The final corrected primary sequence of *T. hirsuta* laccase is given in Fig. 2.

3.2.2. Description of the laccase structure. The *T. hirsuta* laccase fold is similar to the folding pattern of other laccase structures determined to date. The structure can be divided into three sequentially positioned domains. Each domain has a β-pleated sheet structure. Domain 1 (Ala1–Asp128) contains one short α-helix (α1) and two β-sheets. One sheet contains four antiparallel β-strands (β6, β4, β1 and β2) and the other consists of four mixed-type β-strands (β5, β7, β8 and β3). Chains β3 and β8 pack in a collinear fashion. Domain 2 (residues Pro129–Leu308; see Fig. 2) contains two α-helices (α2 and α3) and two β-sheets. One sheet is formed by six antiparallel β-strands (β10, β9, β12, β17, β14 and β15). The second can be described as having a mixed type: it contains five β-strands (β11, β19, β18, β13 and β16). The β11 and β19 strands are parallel to each other.

Domain 3 (residues Val309–Gln499; Fig. 2) is formed by four α-helices and contains one β-hairpin (β21 and β22) and two five-stranded β-sheets. In one β-sheet strands β20, β24, β29, β26 and β27 are antiparallel, while the other β-sheet contains strands β28, β25, β30, β31 and β23 of mixed type (strands β31 and β23 are parallel).

The N- and C-termini form a few hydrogen bonds to neighbouring residues. The main-chain N atom of Ala1 makes a hydrogen bond to the $O^{\delta2}$ atom of Asp142 and the main-chain O atoms of Gln499 form hydrogen bonds to the main-chain N atoms of Lys59 and Ser60.

The laccase structure contains two disulfide bridges. One is formed by cysteines from domains 1 and 3. Cys85 (domain 1) is positioned between α1 and β3 and is bonded to Cys488 from the α8 helix. The second bridge is between domains 1 and 2. Cys117, which is located between β7 and β8, is bonded to Cys205, positioned between β7 and β8. Cys205 S^{γ} has two distinct conformations with approximately equal occupancies.

The protein active site is formed by the substrate-oxidation copper centre T1 (domain 3) and the oxygen-reduction copper cluster T2/T3 positioned in the cavity between domain 1 and domain 3 (Fig. 1).

The Ramachandran plot (Ramakrishnan & Ramachandran, 1965) suggests that all residues except Leu58 are in allowed

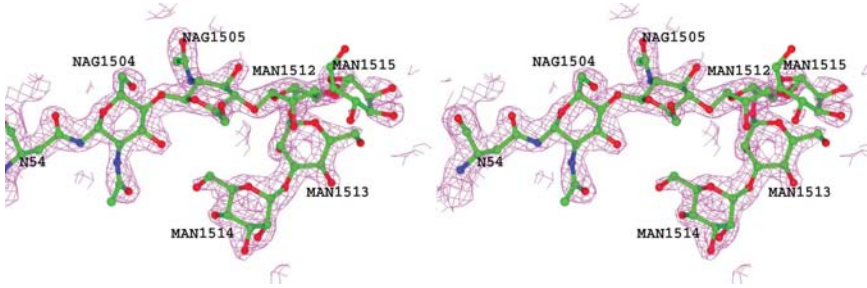

Figure 3
Stereoview of sugar residues bound to Asn54. The $2F_o - F_c$ map shown in pink is contoured at 1σ above the mean.

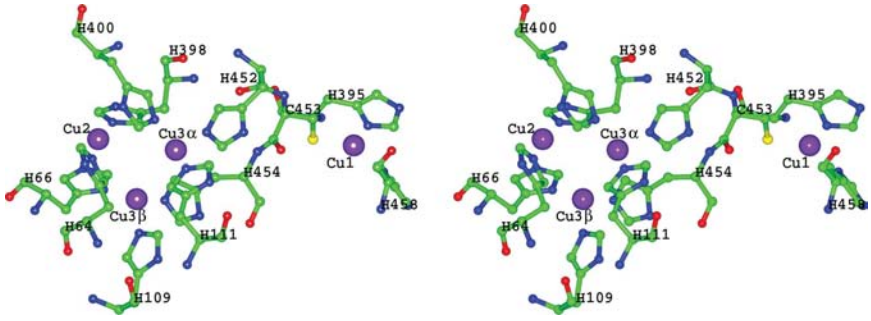

Figure 4
Stereoview of the *T. hirsuta* laccase active site. Cu atoms are shown in violet.

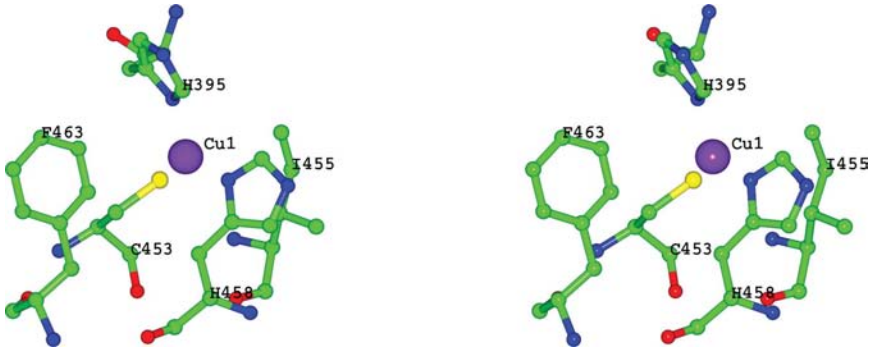

Figure 5
Stereoview of the T1 copper centre.

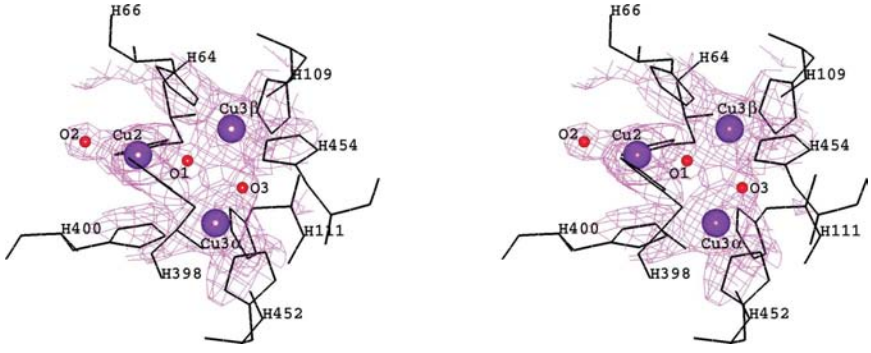

Figure 6
Stereoview of the T2/T3 copper centre.

Table 2
Interatomic distances in the active-site structure of laccase from *T. hirsuta*.

Cu1, T1 centre copper ion; Cu2, T2 centre copper ion; Cu3α, Cu3β, T3 centre copper ions; O3, bridging oxygen ligand for T3 ion pair; O2, T2 centre oxygen ligand; O1, oxygen ligand in the centre of the T2/T3 cluster. *B* denotes the isotropic atomic displacement factor (ADP) and *z* denotes the occupancy values (which are shown in parentheses if not equal to 1.0).

Atom *I* (*z*)	*B* (Å^2)	Atom *J* (*z*)	*B* (Å^2)	*I*–*J* distance (Å)
Cu1 (0.8)	27.5	Cys453 SG	23.8	2.24
		His395 ND1	27.0	2.01
		His458 ND1	24.1	2.05
Cu2 (0.8)	26.9	His64 NE2	22.2	1.96
		His398 NE2	20.7	1.82
		O1 (0.8)	24.8	1.96
		O2	21.9	2.14
Cu3α (0.7)	24.6	His111 NE2	20.3	2.02
		His452 NE2	19.6	2.05
		His400 NE2	21.3	2.02
		O1 (0.8)	24.8	2.71
		O3 (0.8)	21.9	1.75
		His66 ND1	21.5	2.05
Cu3β (0.7)	31.5	His109 NE2	23.1	2.09
		His454 NE2	23.1	2.01
		O1 (0.8)	24.8	2.16
		O3 (0.8)	21.9	2.43
Cu2 (0.8)	26.9	Cu3α (0.7)	24.6	4.10
Cu2 (0.8)	26.9	Cu3β (0.7)	31.5	3.78
Cu3α (0.7)	24.6	Cu3β (0.7)	31.5	3.83

regions. The slightly unusual conformation of Leu58 is stabilized by hydrogen bonds formed by its carbonyl O atom and that of Met57 with the N$^{\varepsilon 2}$ atom of the Gln115 side chain.

During the refinement, 13 sugar (hydrocarbon) residues were included in the model. They bind covalently to Asn54, Asn217, Asn333 and Asn436. Asn217 binds a linear chain of two glucosamine residues (1506 and 1507) and two α-D-mannose residues (1508 and 1521) *via* an *N*-glycosidic bond, while Asn333 binds only one *N*-acetylglucosamine residue (1509). Two residues of *N*-acetylglucosamine (1510 and 1511) form a covalent bond to Asn436. The largest chain of sugar residues binds to Asn54 (Fig. 3). This chain consists of six residues [1504, 1505, 1512 (1515), 1513 and 1514]. The residues of *N*-acetylglucosamine link at the $\beta(1\rightarrow4)$ position. The branching point is positioned on the third residue counting from Asn54, followed by another branching point on α-D-mannose (residue 1513). The α-D-mannose residues are linked by $\alpha(1\rightarrow2)$ and $\alpha(1\rightarrow6)$ bonds, with the third residue from Asn54 (α-D-mannose) giving rise to two more branches. The first branch consists of one α-D-mannose residue, while the second branch consists of two α-D-mannose residues (1513 and 1514) linked to each other at position $\alpha(1\rightarrow3)$ and one additional α-D-mannose residue connected at position $\alpha(1\rightarrow6)$.

Some of the sugar residues (α-D-mannoses 1508, 1514 and 1515) stabilize the laccase crystal structure by the formation of hydrogen bonds and hydrophobic interactions with a symmetry-related protein molecule.

3.2.3. Coordination of the coppers in the active site. The *T. hirsuta* laccase active site consists of the mononuclear T1 copper site and the trinuclear cluster T2/T3 (Malmstrom *et al.*, 1959, 1968, 1969; Solomon, 2006). A substrate-binding pocket containing the T1 copper centre is positioned between domains 2 and 3. The T2/T3 cluster can be found in the cavity between domains 1 and 3. The location of the Cu atoms inside the molecule is shown in Figs. 1 and 4.

Copper ion T1 is coordinated by two histidines, His395 and His458, and one cysteine residue, Cys453 (Fig. 5). The positions of the copper ion and the N and S atoms coordinating the copper belong to the same plane. His395 and His458 interact with the T1 copper ion through N$^{\delta 1}$ atoms at distances of 2.01 and 2.05 Å, respectively. The distance between the Cu1 ion and the S atom of Cys453 is longer at 2.24 Å.

The oxygen-reduction (redox) centre is located deep inside the molecule, approximately 12 Å away from its surface, between domains 1 and 3. This cluster is coordinated by the following amino-acid residues: His64, His66 (β5), His109 (β7), His111, His398 (β25), His400, His452 (β30) and His454. The location of the T2/T3 cluster is 12.2 Å from the T1 centre. The trinuclear cluster T2/T3 is linked to the T1 centre *via* the conserved His452–Cys453–His454 triad (β28), in which Cys453 coordinates copper ion T1 while His452 coordinates the Cu3α ion and His454 interacts with Cu3β (Fig. 4). The three-dimensional structure of the T2/T3 cluster from *T. hirsuta* laccase is shown in Fig. 6. The most important interatomic distances are listed in Table 2. The three copper ions of the T2/T3 cluster form an almost equilateral triangle with distances Cu2—Cu3α = 4.10 Å, Cu2—Cu3β = 3.78 Å and Cu3α—Cu3β = 3.83 Å. An oxygen ligand (O1) has been located in the electron-density map in the centre of the triangle formed by the Cu atoms. The bridging oxygen ligand O3 is positioned between the two coppers of the T3 centre. The distance between O1 and O3 is 2.40 Å, which corresponds to a strong hydrogen-bond distance.

The T3 copper-ion pair is coordinated by six histidine amino-acid residues in the native laccase structure. Five histidine residues interact with copper ions *via* their N$^{\varepsilon 2}$ atoms and the sixth interacts through its N$^{\delta 1}$ atom. The Cu3β ion is coordinated by His66 N$^{\delta 1}$, His109 N$^{\varepsilon 2}$, His454 N$^{\varepsilon 2}$ and O1. The Cu3α ion is coordinated by His111 N$^{\varepsilon 2}$, His400 N$^{\varepsilon 2}$, His452 N$^{\varepsilon 2}$ and O3. Overall, the coordination of the copper sites can be described as distorted tetrahedra.

4. Discussion

In the laccase structure presented, Phe463 is in the axial position in the T1 centre. Residue Leu455 is positioned on the other side of the T1 centre at approximately the same distance (about 3.5 Å). The phenylalanine residue is highly conserved among other high-redox-potential laccases such as those from *T. versicolor* (PDB codes 1gyc and 1kya; Piontek *et al.*, 2002; Bertrand *et al.*, 2002) and *T. maxima* (PDB code 2h5u; Lyashenko, Bento *et al.*, 2006), which suggests that it may act as a binding site for a hydrophobic substrate.

The T1 centre is located in domain 3 and is approximately 6 Å away from the protein surface. The binding of the substrate occurs close to this centre in a substrate-binding pocket formed by loops 161–165, 332–337 and 389–392 and α-helix α9. The substrate-binding pocket has dimensions of 8 ×

10 × 10 Å. Comparison of the amino-acid residues forming the substrate-binding pockets shows that the pockets of high-redox-potential laccases (those from *T. hirsuta* and *T. versicolor*) contain more aromatic residues (about 18 on average) than those of medium-redox-potential laccases (those from *Coprinus cinereus*, *Melanocarpus albomyces* and *Bacillus subtilis*) and low redox-potential ascorbate oxidase (about 13 aromatic residues).

The crystal structure analysis of laccase from *T. versicolor* (PDB code 1kya; Bertrand *et al.*, 2002) cocrystallized with 2,5-xylidine (an analogue of organic substrates) shows that it directly interacts with His458 and Asp206 in the substrate-binding pocket. This Asp206 corresponds to Asn206 in the *T. hirsuta* sequence. Further inspection of the amino-acid sequences of other highly redox-capable laccases, such as those from *T. maxima* and *T. ochracea*, suggests that aspartate is present in the 206th position (Lyashenko, Bento *et al.*, 2006; Lyashenko, Zhukhlistova *et al.*, 2006), as is also the case for laccase from *T. versicolor*. The kinetic parameters of three highly redox-capable laccases were determined by Shleev *et al.* (2004) for the oxidation of several organic substrates. The values of k_{cat} for the laccases from *T. hirsuta*, *T. maxima* and *T. ochracea* were 390, 320 and 80 s^{-1} for catechol; 430, 300 and 90 s^{-1} for guaiacol; 450, 290 and 110 s^{-1} for hydroquinone and 580, 330 and 170 s^{-1} for sinapinic acid (Shleev *et al.*, 2004), respectively. Therefore, the catalytic constants for *T. hirsuta* laccase are much higher than those of the laccases from *T. maxima* and *T. ochracea*. It seems likely that the substitution of aspartate by asparagine plays a key role in the oxidation of organic substrates.

The three-dimensional structure of the T2 centre of *T. hirsuta* laccase (together with the T3 centre) is shown in Fig. 6. The environment of the T2 centre includes His64 $N^{\varepsilon 2}$, His398 $N^{\varepsilon 2}$ and two oxygen ligands, O1 and O2. These four atoms form a flat square. The nature of the O1 and O2 ligands is not yet known (see below). The histidines which coordinate the T2 copper ion form hydrogen bonds to the main-chain atoms of Asp77 and Asp419.

The O1 ligand has been found in the trinuclear centre of laccase from *M. albomyces*, but the T2 centre contained a Cl^- ion instead of O2. The distance to oxygen ligand O1 is about 2.5 Å, suggesting that the atoms interact *via* strong hydrogen bonds. However, in our case these distances are much shorter: Cu2—O2 = 2.14 Å and Cu2—O1 = 1.96 Å. We propose that the O2 and O3 ligands do not represent water molecules. The cluster containing such types of ligands may represent a new intermediate form of laccase.

To date, two possible catalytic mechanisms for the reduction of oxygen to water in the T2/T3 centre have been proposed. The first scheme (Bento *et al.*, 2005) was based on the structural information about laccases that was available at the time. The scheme includes four stages of dioxygen reduction assigned to structurally known intermediates: 'resting' enzyme, two forms of 'resting' enzyme differing in the number and position of bridging hydroxyl groups, fully reduced enzyme and peroxide intermediates. The second scheme (Yoon *et al.*, 2007) was based on the results of spectral analytical investigations of intermediates formed during catalysis and also on density functional theory (quantum-mechanical) calculations. The scheme suggests that in solution laccase can simultaneously exist in the form of a native intermediate (NI), in which a μ_3-oxo ligand (Yoon *et al.*, 2007) is positioned in the centre of T2/T3 copper cluster, and in the so-called 'resting enzyme' state which is formed by double protonation of the native intermediate. Both forms are catalytically active and participate in the first stage of enzymatic catalysis (Yoon *et al.*, 2007). Analysis of the known structures of laccases clearly shows that the laccase from *T. versicolor* (PDB code 1gyc; Piontek *et al.*, 2002) corresponds to the 'resting enzyme' form, while the structure of our laccase from *T. hirsuta* is consistent with the structure of the native intermediate.

This work was financially supported by the Russian Foundation for Basic Research (grant No. 08-04-01558) and the Federal Agency of Science and Innovation RF (Project No. 02.512.12.2002). KMP and OVK thank EMBL Hamburg for access to the EMBL BW7A beamline.

References

Amitai, G., Adani, R., Sod-Moriah, G., Rabinovitz, I., Vincze, A., Leader, H., Chefetz, B., Leibovitz-Persky, L., Friesem, D. & Hadar, Y. (1998). *FEBS Lett.* **438**, 195–200.
Baratto, L., Candido, A., Marzorati, M., Sagui, F., Riva, S. & Danieli, B. (2006). *J. Mol. Catal. B Enzym.*, **39**, 3–8.
Barton, S. C., Pickard, M., Vazquez-Duhalt, R. & Heller, A. (2002). *Biosens. Bioelectron.* **17**, 1071–1074.
Bento, I., Martins, L. O., Lopes, G. G., Carrondo, M. A. & Lindley, P. F. (2005). *Dalton Trans.* **21**, 3507–3513.
Berman, H. M. *et al.* (2002). *Acta Cryst.* D**58**, 899–907.
Bertrand, T., Jolivalt, C., Briozzo, P., Caminade, E., Joly, N., Madzak, C. & Mougin, C. (2002). *Biochemistry*, **41**, 7325–7333.
Collaborative Computational Project, Number 4 (1994). *Acta Cryst.* D**50**, 760–763.
Couto, S. R. & Toca-Herrera, J. L. (2006*a*). *Biotech. Adv.* **24**, 500–513.
Couto, S. R. & Toca-Herrera, J. L. (2006*b*). *Biotechnol. Mol. Biol. Rev.* **1**, 117–122.
Emsley, P. & Cowtan, K. (2004). *Acta Cryst.* D**60**, 2126–2132.
Ferraroni, M., Myasoedova, N. M., Schmatchenko, V., Leontievsky, A. A., Golovleva, L. A., Scozzafava, A. & Briganti, F. (2007). *BMC Struct. Biol.* **7**, 60.
French, S. & Wilson, K. (1978). *Acta Cryst.* A**34**, 517–525.
Gianfreda, L. & Rao, M. A. (2004). *Enzyme Microb. Technol.* **35**, 339–354.
Gianfreda, L., Xu, F. & Bollag, J.-M. (1999). *Bioremediat. J.* **3**, 1–26.
Koroljova (Skorobogat'ko), O., Stepanova, E., Gavrilova, V., Morozova, O., Lubimova, N., Dzchafarova, A., Jaropolov, A. & Makower, A. (1998). *Biotechnol. Appl. Biochem.* **28**, 47–54.
Leonowicz, A. & Grzywnowicz, K. (1981). *Enzyme Microb. Technol.* **3**, 55–58.
Lyashenko, A. V., Bento, I. *et al.* (2006). *J. Biol. Inorg. Chem.* **11**, 963–973.
Lyashenko, A. V., Zhukhlistova, N. E., Stepanova, E. V., Schirwiz, K., Zhukova, Yu. N., Koroleva, O. V., Lamzin, V. S., Zaitsev, V. N., Gabdulkhakov, A. G. & Mikhailov, A. M. (2006). *Crystallogr. Rep.* **51**, 278–285.
Malmstrom, B. G., Finazzi, A. A. & Antonini, E. (1969). *Eur. J. Biochem.* **9**, 383–391.

Malmstrom, B. G., Mosbach, R. & Vanngard, T. (1959). *Nature (London)*, **183**, 321–322.
Malmstrom, B. G., Reinhammar, B. & Vanngard, T. (1968). *Biochim. Biophys. Acta*, **156**, 67–76.
Marzorati, M., Danieli, B., Haltrich, D. & Riva, S. (2005). *Green Chem.* **7**, 310–315.
Messerschmidt, A., Ladenstein, R., Huber, R., Bolognesi, M., Avigliano, L., Petruzzelli, R., Rossi, A. & Finazzi-Agro, A. (1992). *J. Mol. Biol.* **224**, 179–205.
Murshudov, G. N., Vagin, A. A. & Dodson, E. J. (1997). *Acta Cryst.* D**53**, 240–255.
Otwinowski, Z. & Minor, W. (1997). *Methods Enzymol.* **276**, 307–326.
Piontek, K., Antorini, M. & Choinowski, T. (2002). *J. Biol. Chem.* **277**, 37663–37669.
Ramakrishnan, C. & Ramachandran, G. N. (1965). *Biophys. J.* **5**, 909–933.
Read, R. J. (1986). *Acta Cryst.* A**42**, 140–149.
Riva, S. (2006). *Trends Biotechnol.* **24**, 219–226.
Shleev, S., Jarosz-Wilkolazka, A., Khalunina, A., Morozova, O., Yaropolov, A., Ruzgas, T. & Gorton, L. (2005). *Bioelectrochemistry*, **385**, 745–754.
Shleev, S. V., Morozova, O. V., Nikitina, O. V., Gorshina, E. S., Rusinova, T. V., Serezhenkov, V. A., Burbaev, D. S., Gazaryan, I. G. & Yaropolov, A. (2004). *Biochimie*, **86**, 693–703.
Shleev, S., Tkac, J., Christenson, A., Ruzgas, T., Yaropolov, A. I., Whittaker, J. W. & Gorton, L. (2005). *Biosens. Bioelectron.* **20**, 2517–2554.
Solomon, E. I. (2006). *Inorg. Chem.* **45**, 8012–8025.
Solomon, E. I., Baldwin, M. J. & Lowery, M. D. (1992). *Chem. Rev.* **92**, 521–542.
Solomon, E. I., Sundaram, U. M. & Machonkin, T. E. (1996). *Chem. Rev.* **96**, 2563–2605.
Torres, E., Bustos-Jaimes, I. & Le Borgne, S. (2003). *Appl. Catal. B*, **46**, 1–15.
Vagin, A. & Teplyakov, A. (1997). *J. Appl. Cryst.* **30**, 1022–1025.
Yoon, J., Liboiron, B. D., Sarangi, R., Hodgson, K. O., Hedman, B. & Solomon, E. I. (2007). *Proc. Natl Acad. Sci. USA*, **104**, 13609–13614.